THE JOURNAL OF PHYSICAL CHEMISTRY Letters

Letter

pubs.acs.org/JPCL

On Routes to Ultrafast Dissociation of Polyatomic Molecules

Oksana Travnikova,[†] Victor Kimberg,[†,∥] Roberto Flammini,[‡] Xiao-Jing Liu,[†] Minna Patanen,[†] Christophe Nicolas,[†] Svante Svensson,[§] and Catalin Miron*[,†]

[†]Synchrotron SOLEIL, L'Orme des Merisiers, Saint-Aubin, BP 48, F-91192 Gif-sur-Yvette Cedex, France

[‡]IMIP-CNR Istituto di Metodologie Inorganiche e dei Plasmi, 00019 Monterotondo Scalo, Roma, Italy, and

[§]Department of Physics and Astronomy, Uppsala University, Box 516, 75120 Uppsala, Sweden

Supporting Information

ABSTRACT: Dissociation pathways for complex polyatomic molecules can sometimes be obscure due to the multitude of degrees of freedom involved. Here, we suggest the description of a dissociation mechanism implying multimode dynamics on the barrierless potential energy surface. The mechanism is elaborated from the X-ray spectroscopic analysis of the ultrafast nuclear motion in core−shell excited molecules. We infer that in large molecules, dissociation pathways are observed to deviate from the two-body dissociation coordinate due to the internal motion of light linkages, which alters dissociation rates and may yield heavy products on very short time scales. The mechanism is exemplified with the case of 1-bromo-2-chloroethane, where the rotation of the C_2H_4-moiety leads to the dissociation of C−Cl or C−Br bonds in Cl2p or Br3d core-excited states, whose lifetimes last only ∼7 fs.

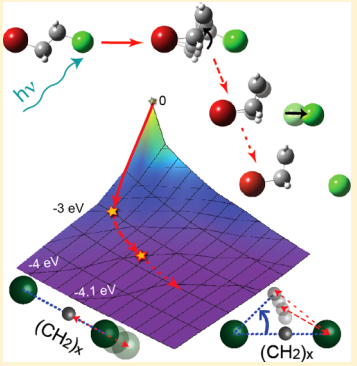

SECTION: Spectroscopy, Photochemistry, and Excited States

Understanding the mechanisms of chemical reactions is the essence of chemistry and the key to their control. However, even the knowledge of dissociation—a simple unimolecular reaction—remains fuzzy, and stimulates the emergence of new concepts, particularly in the case of complex molecules with numerous degrees of freedom. The recent discovery of roaming reactions as an alternative way to describe chemical pathways not covered by the well-established transition state theory is a good case in point.[1] These kinds of reactions have been identified in an increasing number of molecular systems, and have brought into light intriguing questions about the nature of chemical bonds and bond breakage dynamics.[2] In some situations, nature provides us with an intrinsic "molecular timer" to study dissociation. Indeed, when X-rays are used to populate a neutral core-excited state, the very short lifetime of this state (3−8 fs)[3] can set the available time span for the photodissociation process to take place. This ultrafast dissociation (UFD), first shown to take place before electronic relaxation (i.e., Auger decay) of the Br3d→ σ^* core-excited state of HBr,[4] was observed in a number of other molecular systems (e.g., HCl, O_2, H_2O, NH_3, SF_6, CH_3Cl, etc.) as well as in clusters.[5] A simple pseudodiatomic description of UFD, modeling the departing fragments as point-masses and the dissociation along only one coordinate, guided all in-depth studies of the UFD phenomenon to relatively light molecules, where their reduced masses allowed the fragments to travel far enough to reach the complete breakage of the chemical bond during the very short core-hole lifetime. Just as the roaming reaction pathways revealed the unexpected complexity of chemical reactivity, our present discovery of UFD in 1-bromo-2-chloroethane (BCE, $Br(CH_2)_2Cl$) clearly demonstrates the limitation of modeling direct molecular dissociation as a simple one-dimensional bond elongation between two fragments. Here we describe a new dissociation mechanism, involving complex multimode dynamics occurring on a barrierless potential energy surface. The dissociation does not strictly occur along the dissociative C−Cl or C−Br coordinates, but is mediated by the *rotation* of the C_2H_4-moiety.

A fine probe of UFD is resonant photoemission (RPE), where the resonant absorption of an X-ray photon populates final ionic states of the molecule by ejection of an Auger electron of definite energy E_k. RPE spectra allow unambiguous identification of the early electronic decay in the undissociated system (broad molecular features) from the decay taking place in the fragments (sharp atomic features) (see Figure 1).[6]

From the modeling point of view, a lot of advanced computational tools have been developed, which enable one to locate, e.g., conical intersections or transition states.[7,8] Yet accurate modeling requires methods of high computational costs. With the help of quasi-classical models, it was demonstrated that, in the case of UFD, the dissociation rate, and hence the fraction of atomic transitions, decreases with increasing reduced mass. The substitution of H by D in HCl and HBr leads to about 30% decrease in the atomic decay

Received: May 31, 2013
Accepted: June 28, 2013
Published: June 28, 2013

   dx.doi.org/10.1021/jz4011288 | J. Phys. Chem. Lett. 2013, 4, 2361−2366

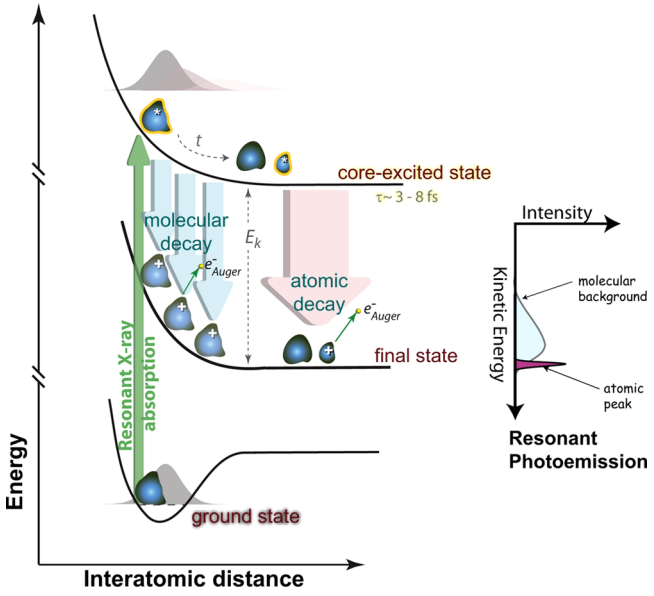

Figure 1. Schematics of the UFD process (left panel) and its manifestation in RPE (right panel). The ground state nuclear wave packet excited to the repulsive intermediate state potential (green arrow) continuously undergoes Auger decay to final ionic states. Owing to the fast nuclear dynamics in the core-excited state, the electronic relaxation can take place at large internuclear distances in the already dissociated atom or fragment (pink arrow), giving rise in the RPE spectra to sharp fragment/atomic lines at kinetic energies (E_k) specific for this fragment/atom. On the contrary, early or fast Auger decay occurring in the undissociated molecule at small internuclear distances (blue arrows) gives rise to broad molecular features for nonparallel potential energy surfaces of core-excited and final ionic states.

contributions relative to the molecular transitions,[9] and no atomic features were observed for Cl_2 at the Cl2p→ σ* resonance, where the dissociation is slow due to the large mass of the fragments.[9]

For molecular systems constituted of more than two atoms, the use of a *pseudodiatomic model* in which each fragment is reduced to a point-mass is quite common, and simple estimates provide a satisfactory description of system's dynamics. Following similar considerations, in the case of larger molecules, such as dichloroethenes ($C_2H_2Cl_2$) or 1-bromo-2-chloroethane, the dissociation is expected to be even slower than in Cl_2 if it proceeds strictly along C−Cl or C−Br bond coordinates.[10] Despite this prediction, the signatures of UFD were recently observed for Cl2p core-excited dichloroethenes.[11] The point-mass model also failed to explain the shorter time scales observed for the strong-field photodissociation of CH_2Br_2.[12] Thus, alternative dissociation pathways must be investigated in the case of complex, polyatomic species enabling bond breakages on unexpectedly short time scales. Here we show that the existence of the $(CH_2)_x$-linkage between heavy atoms plays a crucial role in the nuclear dynamics. The demonstration is given with the example of BCE, which is evidenced to undergo UFD during the lifetime of the Cl2p and Br3d core holes (∼ 7 fs[5]) for both Cl2p/Br3d→ σ* core-excited states.

Figure 2 shows RPE spectra measured at the photon energies corresponding to the excitations at the Cl2p→ σ* and Br3d→ σ* resonant transitions in gas phase BCE. The data have been collected at the soft X-ray PLEIADES beamline at Synchrotron SOLEIL, France. This state-of-the-art spectroscopy facility is briefly described in ref 15 and in the Methods section. In Figure 2, the vertical blue lines mark the positions of the Cl and Br atomic fragment Auger lines, which lie at constant E_k and show nondispersive behavior with the excitation energy.[5,14] The presence of sharp distinct features at these E_k in Figure 2 is a signature of the UFD process occurring in the corresponding core-excited states. Moreover, the overall shape of the RPE spectra, shown in Figure 2b for the region E_k = 175 − 183 eV,

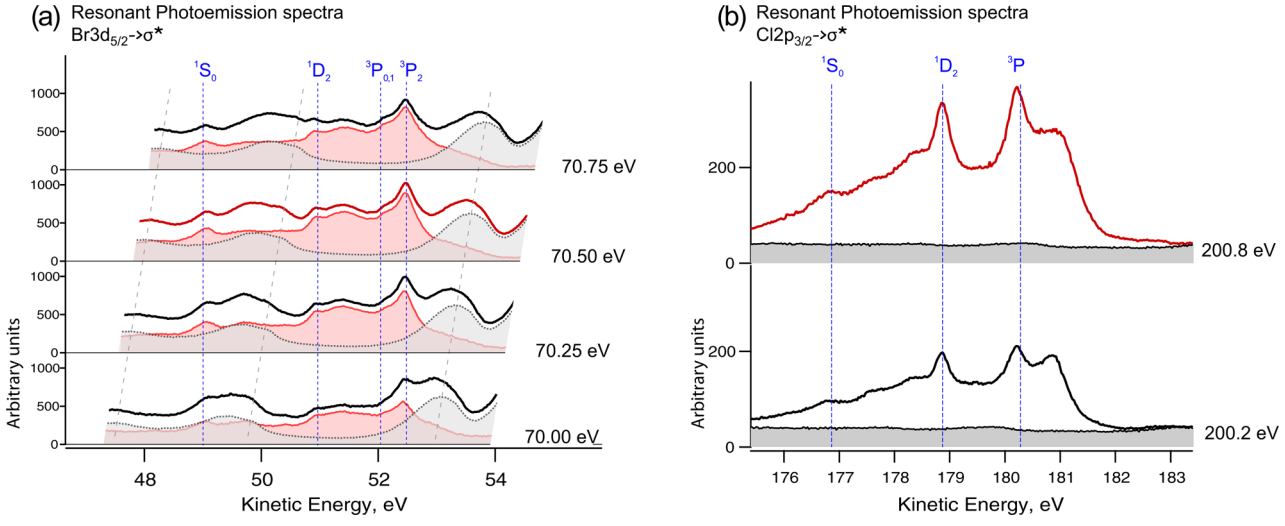

Figure 2. RPE spectra measured at the excitation energies corresponding to the (a) Br3d→ σ* and (b) Cl2p→ σ* transitions. Red curves correspond to the maximum of the photoabsorption cross section within the resonant electronic transition. The gray shaded areas represent the direct photoemission contributions recorded well below the resonant transitions (68 and 198 eV, respectively), and shifted according to the excitation energy of the individual RPE spectra. The red shaded areas in panel "a" are the resonant contributions to RPE estimated by subtraction of the direct photoemission contribution neglecting the interference between direct and resonant contributions.[13] Blue dashed lines mark the positions of the atomic fragment features as observed for HBr[5] and HCl.[14] Gray dashed lines show the dispersive behavior of the molecular features. The electron detection axis is 90° with respect to the X-rays polarization axis.

dx.doi.org/10.1021/jz4011288 | J. Phys. Chem. Lett. 2013, 4, 2361−2366

resembles the RPE spectra of other chlorinated hydrocarbons (such as $C_2H_2Cl_2$ or CH_3Cl), where UFD has been identified before.[11,16]

As an additional confirmation of the existence of UFD in core-excited BCE, we have obtained mass selected resonant photoemission spectra (MS-RPE) by performing energy selected Auger electron−photoion coincidence measurements.[17] The Cl^+/MS-RPE, presented in Figure 3b, clearly

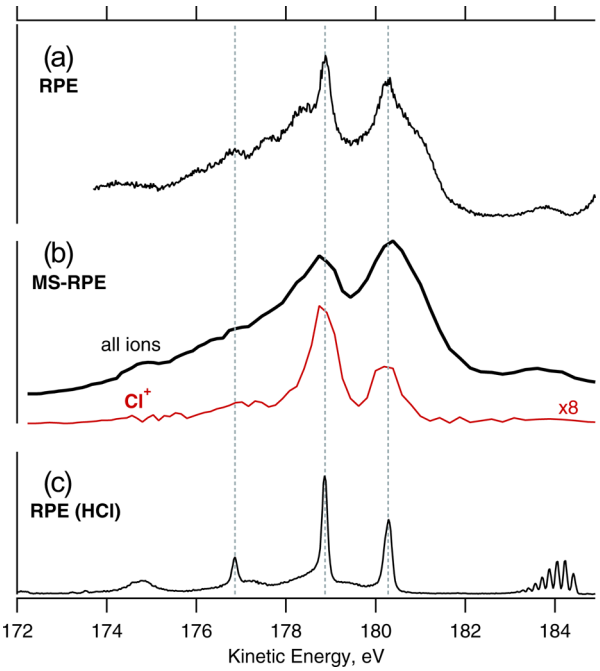

Figure 3. Spectra recorded at the magic angle on top of the Cl2p→ σ^* resonance. (a) High-resolution RPE spectrum of BCE (overall spectral resolution ∼0.08 eV). (b) RPE spectrum of BCE recorded in coincidence with ions without mass selection (black curve) and in coincidence with Cl^+-ions (Cl^+/MS-RPE) (red curve) (overall spectral resolution ∼0.6 eV). (c) High-resolution RPE spectrum of HCl for comparison.

exhibits two sharp lines corresponding to the ^1D and ^3P atomic chlorine states, and a lower intensity peak, which can be assigned to the ^1S atomic state. Moreover, Cl^+ appears nearly exclusively in coincidence with these atomic lines, and their intensities follow the branching ratios of the atomic lines observed in the RPE spectrum of HCl molecule, shown at the bottom of Figure 3 for comparison. This provides a definite proof of the occurrence of UFD in BCE.

In order to gain a qualitative understanding of our observation, we have simulated nuclear relaxation with the eigenvalue-following (EF) algorithm[18] implemented in the Gaussian 09 suite of programs,[19] at the MP2/6-311+G** level of theory. This rather simple modeling was carried out for *trans*- and *gauche*-isomers of BCE. Since at room temperature the *trans*-form is dominant in the gas phase (83%[20]), the discussion will be based on the results for *trans*-BCE. The optimized ground state geometry was used as a starting point for geometry optimization on the excited state potential energy surface using the gradients of the surface. The results show that (i) the BCE molecule undergoes neutral dissociation upon Cl2p/Br3d→ σ^* excitations, and (ii) in the very early stages of the photodissociation, the carbon atoms experience a significant

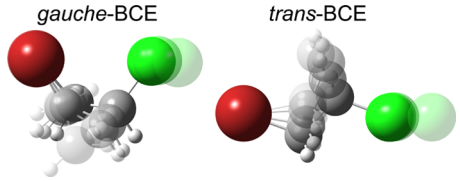

Figure 4. Nuclear relaxation in the Cl2p$^{-1}\sigma^*$ core-excited *gauche*- and *trans*-BCE obtained by gradient-following (EF) simulations. The latest positions of the atoms are shown with the lightest color for comparison with the earliest stages of the relaxation process represented by the two intermediate "frames". Molecular geometries are aligned along the Cl−Br axis, where the position of the Br atom is fixed.

displacement while the halogen atoms remain nearly still (Figure 4).

Additionally, we compared classical trajectories computed for Cl2p and Br3d core-excited BCE using the Atom Centered Density Matrix Propagation (ADMP) molecular dynamics model[21] with the ones for core-excited HCl*, Cl_2, and CH_3Cl* for Cl2p and with HBr*, Br_2, and CH_3Br* for Br3d. The results, presented in Figure 5 for Cl2p excitation, show that the

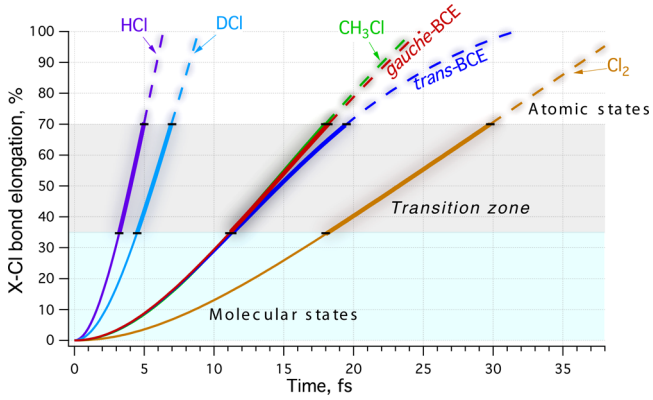

Figure 5. ADMP classical trajectory simulations for Cl2p core-excited BCE, HCl*, Cl_2, and CH_3Cl* molecular systems.

dissociation of the C−Cl* and C−Br* bonds proceeds at nearly the same speed in BCE as in CH_3Cl* and CH_3Br*, respectively, where UFD has been previously observed, as expected for considerably lower reduced masses of compounds.[16,22] ADMP classical trajectory simulations also show large movements of the carbon atoms as mentioned above.

The significant displacement of the carbon atoms in the beginning of the nuclear relaxation in the core-excited states of BCE can be described as a *rotation* of the C_2H_4-linkage around the second halogen atom (Figure 4). A similar motion can be modeled by the combination of three ground state normal vibrational modes, which are dominated by motions of the carbon atoms and therefore possess low reduced masses (see Supporting Information Figure S1). An exact picture of the nuclear dynamics can only be obtained by calculating the multidimensional potential energy surfaces involving all 18 normal vibrational modes of BCE, which, computationally, would be an extremely challenging task. To avoid this complexity, we identified two coordinates leading to the dissociation of the halogen atom: (1) the detachment of the core-excited halogen, where Cl−Br distance serves as a reference for the separation of the fragments; (2) the rotation of the C_2H_4-moiety around the second halogen atom, which

dx.doi.org/10.1021/jz4011288 | J. Phys. Chem. Lett. 2013, 4, 2361−2366

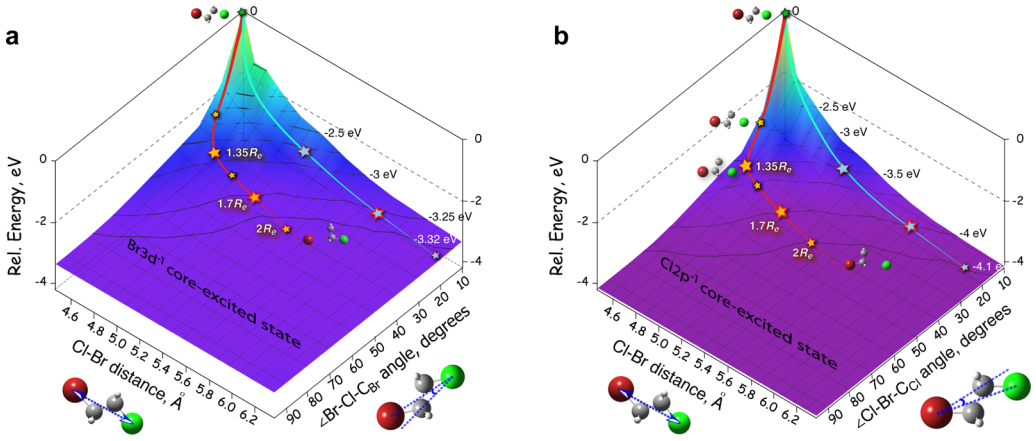

Figure 6. Potential energy surfaces for the core-excited states of BCE. (a) Br3d$^{-1}\sigma^{*1}$. (b) Cl2p$^{-1}\sigma^{*1}$. The potential energy surfaces are calculated along the Cl−Br distance and the angle Br−Cl−C(Br) for "a", and Cl−Br−C(Cl) for "b". All the other coordinates were optimized at each point of the potential energy surface scans. Yellow stars mark the gradient-following geometry optimization path of the core-excited states, which are mapped on these potential energy surfaces by corresponding coordinates. Blue curves show the trajectories that would be followed if the Br/Cl-atom were to separate from the residual fragment by moving apart along the C−Br/C−Cl bond. Blue stars correspond to the bond lengths of 1.35*R_e, 1.7*R_e and 2*R_e, where R_e is the C−Br and C−Cl equilibrium bond distances in panels "a" and "b", respectively.

leads to the angle change between the C−Cl (or C−Br) and the Cl−Br axis. While the coordinate (1) can be approximated by the pseudodiatomic model and a two-body dissociation (X_{Cl}−$Y_{C_2H_4Br}$ or X_{Br}−$Y_{C_2H_4Cl}$), the rotation of the C_2H_4-linkage appears to be a multimode dynamical mechanism and should be seen as an alternative dissociation pathway.

Three-dimensional (3D) potential energy surfaces of the Cl2p$^{-1}\sigma^*$ and Br3d$^{-1}\sigma^*$ core-excited states are presented in Figure 6, which shows that dissociation can be achieved in the core-excited states independently, either by (1) the detachment of the halogen atom or by (2) the motion of the C_2H_4-group. However, the shortest paths to reach the valley of the potential energy surfaces of the core-excited states require both coordinates. The slope appears to be steeper along the C_2H_4-rotation coordinate for core-excited state geometries not far from the ground state equilibrium geometry. This selects C_2H_4-rotation as the main dissociation mechanism, at least during the early stages of the photodissociation. Moreover, the significantly lower reduced mass of the C_2H_4-motion, as compared to the Cl−Br relative displacement, enables considerably faster dynamics along the rotation coordinate. The latter is crucial for entering in a few fs time scale to the dissociation transition zone, where well-defined energy levels of the excited molecule do not exist anymore and atomic orbitals start to form[34] (see Supporting Information). These results suggest that UFD is possible in the Cl2p$^{-1}\sigma^*$ and Br3d$^{-1}\sigma^*$ core-excited states owing to the internal motion of the carbon atoms, and requiring only short distances to be traveled by the heavy fragments to achieve dissociation.

In conclusion, the unexpected UFD process observed in BCE can be explained by the low-reduced-mass motion of the C_2H_4-moiety allowing the C−Cl/C−Br bond breakage within the short lifetime of the Cl2p/Br3d core-excited states. Both C_2H_4-rotation and C−Cl/C−Br bond stretching participate in the dissociation process, but the rotation plays a crucial role at the very beginning, and the dissociation process without rotation would be by far slower. We expect this multimode dissociation pathways to be rather general in complex core-excited systems with many degrees of freedom, and particularly favored in systems with light $(CH_2)_x$-linkages, where low-reduced-mass vibrational modes enable ultrafast nuclear dynamics. Steric hindrance (e.g., in *trans*-isomers as compared to *cis*- or *gauche*-isomers) and/or additional substituents on $(CH_2)_x$-linkage would serve as adverse factors slowing down the dissociation process. This observation sheds new light on the essence of UFD mechanisms in core-excited states and reveals complex nuclear dynamics occurring via multimode pathways. An attractive complementary approach to reach a deeper understanding for these dissociation dynamics would be time-resolved electron spectroscopy using a pump/probe scheme based on ultrashort pulses obtained by high harmonic generation or at the XUV free electron lasers.

METHODS

The experiment was performed at the PLEIADES beamline[15,23−25] at the SOLEIL synchrotron in Saint-Aubin, France. The beamline covers the 9−1000 eV energy range, with any type of polarization. Monochromatic light is obtained from a plane grating monochromator with no entrance slit. The RPE measurements were performed using a VG-Scienta R4000 electron spectrometer equipped with a differentially pumped gas cell and mounted with the electron detection axis vertical. X-rays polarization was set at two configurations: (1) at the magic angle of 54.7° with respect to this axis to avoid electron emission anisotropy effects, and (2) at 90° to suppress direct photoemission contributions[5,14] and hence maximize the RPE relative weight in the spectra. The monochromator slit was 400 μm, corresponding to a photon bandwidth better than 15 meV at 70 eV and 80 meV at 200 eV. The electron spectrometer was operated at 100 eV pass energy with a slit of 300 μm providing a kinetic energy resolution of 75 meV. The multicoincidence experiment was performed with the dedicated double-toroidal electron analyzer (DTA), described in detail elsewhere,[26−28] facing a conventional time-of-flight (TOF) mass spectrometer.[29,30] The electron detection axis of the DTA was set to the magic angle of 54.7° with respect to the **e** vector of the light polarization. The DTA was operated at a 80 eV pass energy providing a kinetic energy resolution of ∼0.6 eV.

1,2-Bromochloroethane (99.5%) from Sigma-Aldrich was additionally purified by several freeze−pump−thaw cycles. The

dx.doi.org/10.1021/jz4011288 | J. Phys. Chem. Lett. 2013, 4, 2361−2366

pressure of the sample in the vacuum chambers was kept constant around 2.5×10^{-6} mbar.

All simulations were carried out with Gaussian 09 suite of programs[19] with the 6-311+G** basis set. The absence of a core electron in the Br3$d^{-1}\sigma^{*1}$ and Cl2$p^{-1}\sigma^{*1}$ core-excited states was simulated with the equivalent core model (ECM) approximation.[31−33] Ground state geometry optimization, vibrational analysis, and 3D potential energy surface scans were performed at the MP2 level of theory. Classical trajectory calculations with the ADMP molecular dynamics model were performed at the HF level of theory. 3D potential energy surfaces were obtained by restricted scans along the two coordinates indicated in (Figure 6), with 0.1 Å and 10° increments. All other coordinates were optimized at each step of the scans.

■ ASSOCIATED CONTENT

Supporting Information

See Supporting Information for extended discussion. This material is available free of charge via the Internet at http://pubs.acs.org/.

■ AUTHOR INFORMATION

Corresponding Author

*E-mail: Catalin.Miron@synchrotron-soleil.fr.

Present Address

[‖]Center for Free-Electron Laser Science, Notkestrasse 85, 22607 Hamburg, Germany.

Notes

The authors declare no competing financial interest.

■ ACKNOWLEDGMENTS

This work was supported by FP7/2007-2013 Grant No. 252781 (O.T.) and Triangle de la Physique Contract No. 2007-010T (O.T., S.S.). Data collection was performed at the PLEIADES beamline at the SOLEIL Synchrotron, France (proposal numbers 20090655, 20110467, 20111116). We thank E. Robert for technical assistance and the SOLEIL staff for stable operation of the equipment and storage ring during the experiments. Ph. Martinez is warmly acknowledged for his kind support in the installation of the simulation software packages on SOLEIL calculation cluster.

■ REFERENCES

(1) Townsend, D.; Lahankar, S. A.; Lee, S. K.; Chambreau, S. D.; Suits, A. G.; Zhang, X.; Rheinecker, J.; Harding, L. B.; Bowman, J. M. The Roaming Atom: Straying from the Reaction Path in Formaldehyde Decomposition. *Science* **2004**, *306*, 1158−1161.

(2) Bowman, J. M.; Shepler, B. C. Roaming Radicals. *Annu. Rev. Phys. Chem.* **2011**, *62*, 531−553.

(3) Nicolas, C.; Miron, C. Lifetime Broadening of Core-Excited and -Ionized States. *J. Electron Spectrosc. Relat. Phenom.* **2012**, *185*, 267−272.

(4) Morin, P.; Nenner, I. Atomic Autoionization Following Very Fast Dissociation of Core-Excited HBr. *Phys. Rev. Lett.* **1986**, *56*, 1913−1916.

(5) Morin, P.; Miron, C. Ultrafast Dissociation: An Unexpected Tool for Probing Molecular Dynamics. *J. Electron Spectrosc. Relat. Phenom.* **2012**, *185*, 259−266.

(6) Miron, C.; Morin, P. High-Resolution Inner-Shell Photoionization, Photoelectron and Coincidence Spectroscopy. In *Handbook of High-Resolution Spectroscopy*; Quack, M., Merkt, F., Eds.; John Wiley & Sons, Ltd: Chichester, U.K., 2011; pp 1655−1690.

(7) Plasser, F.; Barbatti, M.; Aquino, A. A.; Lischka, H. Electronically Excited States and Photodynamics: A Continuing Challenge. *Theor. Chem. Acc.* **2012**, *131*, 1073.

(8) Matsika, S.; Krause, P. Nonadiabatic Events and Conical Intersections. *Annu. Rev. Phys. Chem.* **2011**, *62*, 621−643.

(9) Kukk, E. Nuclear Dynamics and Electronic Structure of Molecules by Resonant Auger Spectroscopy. *J. Electron Spectrosc. Relat. Phenom.* **2002**, *127*, 43−51.

(10) The slopes of Cl2p core-excited states in HCl, Cl_2, CH_3Cl, $C_2H_2Cl_2$ and $Br(CH_2)_2Cl$ and the slopes of Br3d core-excited states in HBr, CH_3Br and $Br(CH_2)_2Cl$ are comparable [this work]. Therefore considerations of extremely repulsive states in the case of $C_2H_2Cl_2$ and $Br(CH_2)_2Cl$ can be excluded.

(11) Céolin, D.; Travnikova, O.; Bao, Z.; Kivimäki, A.; Carniato, S.; Piancastelli, M. Effect of the Cl2p Core Orbital Excitation on the Nuclear Dynamics of the Three Dichloroethylene Isomers. *J. Electron Spectrosc. Relat. Phenom.* **2011**, *184*, 24−28.

(12) Loh, Z.-H.; Leone, S. R. Ultrafast Strong-Field Dissociative Ionization Dynamics of CH_2Br_2 Probed by Femtosecond Soft X-ray Transient Absorption Spectroscopy. *J. Chem. Phys.* **2008**, *128*, 204302.

(13) Feifel, R.; Burmeister, F.; Sałek, P.; Piancastelli, M. N.; Bässler, M.; Sorensen, S. L.; Miron, C.; Wang, H.; Hjelte, I.; Björneholm, O.; Naves de Brito, A.; Gel'mukhanov, F. K.; Ågren, H.; Svensson, S. Observation of a Continuum−Continuum Interference Hole in Ultrafast Dissociating Core-Excited Molecules. *Phys. Rev. Lett.* **2000**, *85*, 3133−3136.

(14) Kivimäki, A.; Kukk, E.; Karvonen, J.; Mursu, J.; Nõmmiste, E.; Aksela, H.; Aksela, S. Angular Distribution of Electronic Decay Following Molecular and Rydberg Excitations at the Cl 2*p* Edge of HCl. *Phys. Rev. A* **1998**, *57*, 2724−2730.

(15) Miron, C.; Nicolas, C.; Travnikova, O.; Morin, P.; Sun, Y.; Gel'mukhanov, F.; Kosugi, N.; Kimberg, V. Imaging Molecular Potentials Using Ultrahigh-Resolution Resonant Photoemission. *Nat. Phys.* **2012**, *8*, 135−138.

(16) Miron, C.; Morin, P.; Céolin, D.; Journel, L.; Simon, M. Multipathway Dissociation Dynamics of Core-Excited Methyl Chloride Probed by High Resolution Electron Spectroscopy and Auger-Electron-Ion Coincidences. *J. Chem. Phys.* **2008**, *128*, 154314.

(17) Miron, C.; Morin, P. High-Resolution Inner-Shell Coincidence Spectroscopy. *Nucl. Instrum. Methods Phys. Res., Sect. A* **2009**, *601*, 66−77.

(18) Banerjee, A.; Adams, N.; Simons, J.; Shepard, R. Search for Stationary Points on Surfaces. *J. Phys. Chem.* **1985**, *89*, 52−57.

(19) Frisch, M. J.; Trucks, G. W.; Schlegel, H. B.; Scuseria, G. E.; Robb, M. A.; Cheeseman, J. R.; Scalmani, G.; Barone, V.; Mennucci, B.; Petersson, G. A. et al. *Gaussian 09*, revision A.02; Gaussian Inc.: Wallingford, CT, 2009.

(20) Tanabe, K. Calculation of Infrared Band Intensities and Determination of Energy Differences of Rotational Isomers of 1,2-Dichloro-, 1,2-Dibromo- and 1-Chloro-2-Bromoethane. *Spectrochim. Acta A* **1972**, *28*, 407−424.

(21) Schlegel, H. B.; Iyengar, S. S.; Li, X.; Millam, J. M.; Voth, G. A.; Scuseria, G. E.; Frisch, M. J. Ab Initio Molecular Dynamics: Propagating the Density Matrix with Gaussian Orbitals. III. Comparison with Born−Oppenheimer Dynamics. *J. Chem. Phys.* **2002**, *117*, 8694−8704.

(22) Olney, T. N.; Chan, W. F.; Cooper, G.; Brion, C.; Tan, K. The Complete Valence Shell Photoelectron Spectra of CH_3F, CH_3Cl, and CH_3Br Using Synchrotron Radiation at hv = 72 eV: A Comparison with Many-Body Greens Function Calculations. *J. Electron Spectrosc. Relat. Phenom.* **1993**, *66*, 83−100.

(23) Travnikova, O.; Liu, J.-C.; Lindblad, A.; Nicolas, C.; Söderström, J.; Kimberg, V.; Gel'mukhanov, F.; Miron, C. Circularly Polarized X Rays: Another Probe of Ultrafast Molecular Decay Dynamics. *Phys. Rev. Lett.* **2010**, *105*, 233001.

(24) Söderström, J.; Lindblad, A.; Grum-Grzhimailo, A. N.; Travnikova, O.; Nicolas, C.; Svensson, S.; Miron, C. Angle-Resolved Electron Spectroscopy of the Resonant Auger Decay in Xenon with meV Energy Resolution. *New J. Phys.* **2011**, *13*, 073014.

(25) Lindblad, A.; Kimberg, V.; Söderström, J.; Nicolas, C.; Travnikova, O.; Kosugi, N.; Gel'mukhanov, F.; Miron, C. Vibrational Scattering Anisotropy in O_2 − Dynamics Beyond the Born−Oppenheimer Approximation. *New J. Phys.* **2012**, *14*, 113018.
(26) Miron, C.; Simon, M.; Leclercq, N.; Morin, P. New High Luminosity "Double Toroidal" Electron Spectrometer. *Rev. Sci. Instrum.* **1997**, *68*, 3728−3737.
(27) Guen, K. L.; Céolin, D.; Guillemin, R.; Miron, C.; Leclercq, N.; Bougeard, M.; Simon, M.; Morin, P.; Mocellin, A.; Burmeister, F.; de Brito, A. N.; Sorensen, S. L. Development of a Four-Element Conical Electron Lens Dedicated to High Resolution Auger Electron−Ion(s) Coincidence Experiments. *Rev. Sci. Instrum.* **2002**, *73*, 3885−3894.
(28) Liu, X.-J.; Nicolas, C.; Miron, C. Design of a Lens Table for a Double Toroidal Electron Spectrometer. *Rev. Sci. Instrum.* **2013**, *84*, 033105.
(29) Morin, P.; Simon, M.; Miron, C.; Leclercq, N.; Hansen, D. L. Electron−Ion Spectroscopy: A Probe of Molecular Dynamics. *J. Electron Spectrosc. Relat. Phenom.* **1998**, *93*, 49−60.
(30) Céolin, D.; Miron, C.; Simon, M.; Morin, P. Auger Electron−Ion Coincidence Studies to Probe Molecular Dynamics. *J. Electron Spectrosc. Relat. Phenom.* **2004**, *141*, 171−181.
(31) Dow, J. D.; Franceschetti, D. R.; Gibbons, P. C.; Schnatterly, S. E. Soft X-ray Threshold Shapes Extracted from Linde's Rule in the Optical Alchemy Approximation. *J. Phys. F* **1975**, *5*, L211−L216.
(32) Chen, C. T.; Ma, Y.; Sette, F. *K*-Shell Photoabsorption of the N_2 Molecule. *Phys. Rev. A* **1989**, *40*, 6737−6740.
(33) Adachi, J.; Kosugi, N.; Shigemasa, E.; Yagishita, A. Renner-Teller Splitting in the C 1s → π^* Excited States of CS_2, OCS, and CO_2. *J. Chem. Phys.* **1997**, *107*, 4919−26.
(34) Wernet, P.; Odelius, M.; Godehusen, K.; Gaudin, J.; Schwarzkopf, O.; Eberhardt, W. Real-Time Evolution of the Valence Electronic Structure in a Dissociating Molecule. *Phys. Rev. Lett.* **2009**, *103*, 013001.